Humanoid Walking Robot: Modeling, Inverse Dynamics, and Gain Scheduling Control

Elvedin Kljuno and **Robert L. Williams II**
Department of Mechanical Engineering
Ohio University, Athens, OH 45701

Revised Manuscript Submitted to:
Journal of Robotics
Hindawi Publishing Corporation
May, 2010

Keywords: humanoid robot, bipedal walking, joint torques, ground force, inverse dynamics, tracking error linearization control.

ABSTRACT

This article presents an overview of bipedal walking models by grouping them into two categories: models with concentrated mass and models with distributed mass. As an example of the models with concentrated mass, a mass-spring inverted pendulum model is presented, accompanied by an analysis. As an example of a more complex distributed mass model, a 10-dof walking robot model is developed and analyzed, including the model kinematics, dynamics and controls, with numerical solution simulations for desired joint trajectories, recorded from real human walking cycle data. Kinematic and dynamic analysis is discussed including results for joint torques and ground force necessary to implement the prescribed walking motion. This analysis is accompanied by a comparison with available experimental data. Finally, an inverse plant and tracking error linearization based controller design approach is described, accompanied by results analysis and conclusions about controller performance. The main contribution of this article is presentation of a novel combination of nonlinear gain scheduling with a concentrated mass model for a MIMO bipedal robot system.

Corresponding author:
Robert L. Williams II, Professor
Department of Mechanical Engineering
259 Stocker Center, Ohio University
Athens, OH 45701-2979
Phone: (740) 593-1096
Fax: (740) 593-0476
E-mail: williar4@ohio.edu
URL: oak.cats.ohiou.edu/~williar4

1. INTRODUCTION

Modeling of human body walk has been evolved from simple models such as an inverted pendulum model [1, 10, 11] and mass-spring model [2, 12] to relatively complicated models that include relatively high number of degrees of freedom [5-8, 13]. Primary goal of those models is to predict the internal and external forces during a regular walking cycle. Detailed human body models can include calculations of the most important muscle forces for particular types of motion. However, for a robot that is actuated via rotational motors, calculation of particular muscle forces is not needed, but the moments they produce about the corresponding joints. There are two main reasons for the calculation of the joint torques:

(a) Based on a walking model one can predict maximum torques that are necessary to generate particular motion of a robotic structure. The maximum torque and maximum power are necessary data to choose joint actuators. The procedure of the actuators (motors) selection based on the robot dynamic model is inherently iterative, since the mass distribution and consequently, the static and dynamic forces are significantly dependent on the sizes and locations of the chosen actuators.

(b) Torques at relevant joints for particular motion, calculated based on a walking model, can be used to generate nominal control trajectories for a complex walking robotic architecture. Those nominal trajectories can be calculated offline or in real-time using an inverse plant model. The advantage of the later is that the reference (desired) trajectories can be changed online depending on the conditions imposed by environment rather than relaying on the pre-calculated reference trajectories. This is essential for obstacle avoidance, which requires that the reference trajectories are adjusted accordingly.

Inclusion of more degrees of freedom in a walking robot model normally leads to more precise results, but also it leads to more efforts needed to understand the process and what is happening with internal variables in the robotic structure. The next sections give an overview of the simplified models and general features of a more complex model.

This paper presents a reference model based control design for a 10 Degrees of Freedom (DOF) bipedal walking robot, using nonlinear gain scheduling. The main goal of this work is to show how a concentrated mass model of bipedal walkers can be used as a reference model for prediction of the required joint torques for a bipedal walking robot. A relatively complicated architecture, high DOF, and balancing requirements make the control task of these robots very difficult. Although traditional linear control techniques, such as a PID controller and variants, can be used to control bipedal robots, nonlinear control approaches are necessary for higher performance requirements.

Nonlinear control systems are based on the error dynamics, which requires calculation of nominal values of the control inputs and nominal state variables, which can be obtained using an inverse (reference system) system. However, the problem that arises is that an exact dynamic inverse is impossible to obtain in the general case. Instead a pseudoinverse is used. The second problem is that the dynamic pseudoinverse regularly requires stabilization [14].

The main contribution of this work is to show that the reference model can be a bipedal walking model with concentrated mass at the center of gravity, which removes the problems related to design of a pseudoinverse system. Another significance of this approach is the reduced calculation requirements due to a simplified procedure of nominal joint torques calculation.

Since a concentrated mass model is used as a reference model for obtaining the nominal torques, a comparable overview of walking models is given by grouping them into two overall groups: models with the concentrated mass and models with distributed mass. Specifically, the mass-spring inverted pendulum model is described with emphasis on how to adjust this model to be used for the torques/forces prediction in complex bipedal walking architectures. Finally, simulation of the concentrated mass model based control is shown in the case of a 10 DOF walking robot model, including kinematics, dynamics, and controls accompanied with numerical solutions for particular desired joint trajectories, recorded from real human walking cycle data.

Kinematic and dynamic analysis is discussed including results for joint torques and ground force necessary to implement the prescribed walking motion. This analysis is accompanied with a limited comparison with available experimental data. Finally, an inverse plant and tracking error linearization based controller design approach is described accompanied with results analysis and conclusions about the controller performance.

To our knowledge, the nonlinear gain scheduling based on a concentrated mass model has not been applied to control a bipedal robot. Moreover, it is difficult to find any sources covering the nonlinear gain scheduling for a bipedal robot control. This should not be confused with a PID gain scheduled controller. The nonlinear gain scheduled controller specifically designed for the bipedal robot has the gains scheduled based on the nonlinear model and provides significantly better performance than a PID gain scheduled controller. The drawback side of this approach is extremely difficult design process since the system is a MIMO system (Multiple Inputs, Multiple Outputs) and there are significant couplings between the control paths from different control inputs (joints torques) to different outputs (the joints angles and corresponding derivatives).

Despite the complicated controller design, there are several significant advantages of using this method that justify using the nonlinear gain scheduling method instead of a simple PID controller. The most important advantages of this approach are the high tracking performance (low trajectories tracking errors) which cannot be achieved using traditional PID

techniques and higher maximum velocities of a bipedal robot accompanied with better balancing. Moreover, traditional control techniques, such as PID, treat each joint separately, and cross coupling between different inputs-output paths is considered as disturbances, which limits achievable performance of such control systems. That is, by treating the system as a full MIMO system, the controller performance can be significantly better than assuming decoupling and hoping that the disturbances will be sufficiently small, such that the control system can still track the desired trajectories.

In this article we propose a novel combination of a nonlinear gain scheduling with a concentrated mass model for the MIMO bipedal robot system.

1.1 Models with Concentrated Mass

The group of relatively simple walking models is based on the inverted pendulum structure with variations combining a spring or two springs and dampers. The simple models include one or two variables with overall mass concentrated into a point, a center of mass (COM).

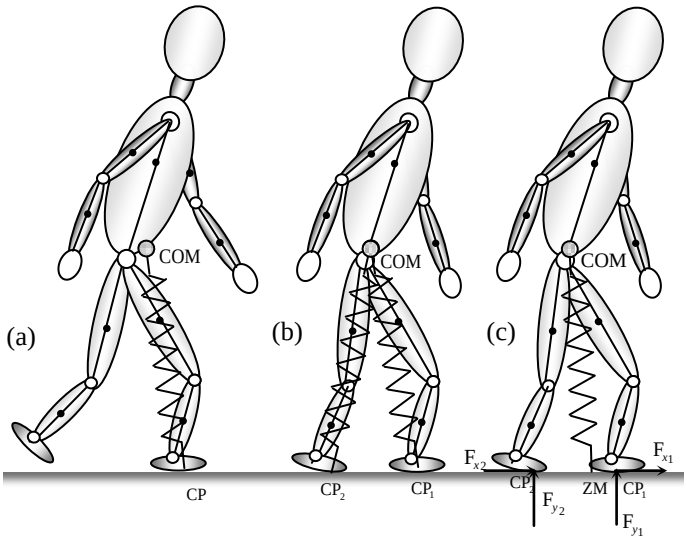

Figure 1. Mass and spring inverted pendulum walking gait representation: (a) single support, (b) double support represented by two springs, (c) double support represented by a single spring.

The Six Determinants model [1] has been used in the past to analyze the human gait cycle. Due to inconsistency with theoretical and experimental results, this model has been replaced by the Inverted Pendulum model, which gives results much closer to those obtained experimentally. One of the major inconsistencies of the regular Inverted Pendulum model results with the experimental results is the zero energy input, which means that the model does not consider the energy lost during the gait cycle.

A more advanced, but still one of the simplest models for human gait analysis is Mass and Spring Inverted Pendulum (MSIP) model [2]. The point mass is equal to the total mass of the body concentrated into the center of gravity. The spring connects the ground contact point (the center of pressure CP) and the center of gravity (CG) and its deflections include all changes of the distance between the CP and the CG points due to flexions/extensions of the hip, knee and ankle joints. Figure 1 shows the concept of representing a complex human body (or a bipedal robot) by a mass and spring model.

The spring connects the center of pressure (CP) and the center of mass (COM) (a). The COM point can be considered as very close to the hips since its position varies relatively close to the hip joint during the walking cycle. The double support period (b) can be modeled using mass and two springs connecting the COM and centers of pressures CP1 and CP2. However, double support period is relatively short compared to the duration of the gait cycle and frequently can be considered as instantaneous. Besides this case, a single spring model can cover a double support period in the way of interpreting the spring-ground connection as a zero moment (ZM) point (c). In other words, the total moment of F_{y1} and F_{y2} forces for ZM point is equal to zero. A state space representation of the simple mass-spring inverted pendulum, shown in Figure 2, is:

$$\begin{bmatrix} \dot{x}_1 \\ \dot{x}_2 \\ \dot{x}_3 \\ \dot{x}_4 \end{bmatrix} = \begin{bmatrix} \dot{r} \\ \ddot{r} \\ \dot{\theta} \\ \ddot{\theta} \end{bmatrix} = \begin{bmatrix} x_2 \\ x_1 x_4^2 - g\cos(x_3) + \frac{k}{m}(l_0 - x_1) - \frac{b}{m}x_1^2 \\ x_4 \\ (g\sin(x_3) - 2x_2x_4)/x_1 + \frac{\tau}{mx_1^2} \end{bmatrix} \quad (1)$$

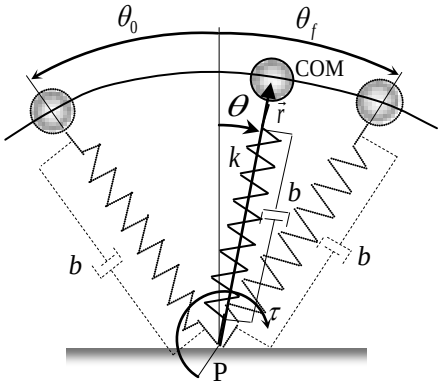

Figure 2. Mass-spring inverted pendulum model

where x_1 represents the radial distance of the COM from the ground contact point, x_2 is the radial velocity, x_3 is the angular velocity of the link between the ground contact and the COM, which is approximately equal to the angular velocity of the stance leg during the single support phase of the walking, and x_4 is the corresponding angular acceleration.

The state space differential equation (1) can be used to solve for the trajectory of the center of mass, as well as the ground

reaction and the spring forces. The trajectory obtained using this model approximates the trajectory of a real bipedal system's center of mass. Similarly, force plate measurements [9] show that the ground reaction force of a real bipedal system can be approximated by the force calculated using (1).

Besides use of this model for studying different parameters of the walking cycle mechanical energy optimization by biological systems, the significance of this result is reflected in the fact that this model with concentrated mass can be used as an approximate reference model for complex robotic bipedal systems control.

The idea is to construct a mathematical model based on the equation set (1) to calculate the reaction force repeatedly at specified time steps and use that result to calculate required torques for a complex architecture bipedal robotic system such that total reaction force is equal to the one obtained by the concentrated mass model. The block diagram of this control system concept is shown in Figure 3. One of the main advantages of this reference model is the possibility for dynamic system inversion without facing the issues of the inverse system stabilization [14].

Namely, the main problem of using dynamic inversion system to calculate the nominal control input vector is the difficulty of designing the exact causal inversion resulting in replacing the a pseudoinverse system that very often needs to be stabilized. In this case of the inverse system, when the model with concentrated mass is used for nominal input prediction, there is no need for stabilization.

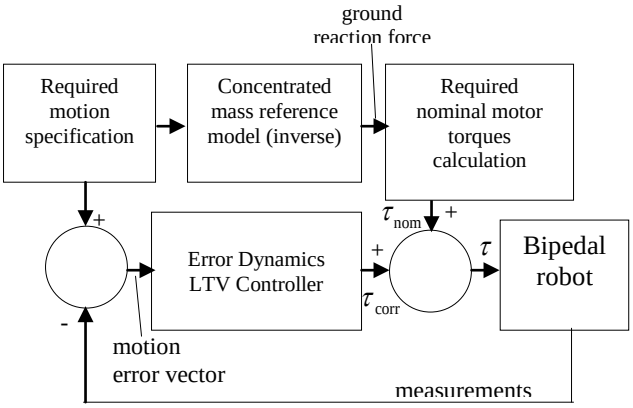

Figure 3. Control system architecture based on the torque prediction using the concentrated mass reference model

In Figure 3, τ_{nom} is the nominal torque vector calculated based on the ground force provided by the reference model (mass-spring model), τ_{corr} is the correction calculated based on the measurements of the robot joints angles and acceleration vector, and τ is the commanded torque signal that is sent to the actuators.

The model includes damping represented by the coefficient b and a torque τ for the case when the center of pressure at a foot is not taken as a spring - ground contact point. The ground contact force that occurs during human walking can be predicted using the mass-spring model.

Potential energy accumulated in the spring and the gravitational potential energy interchange with the kinetic energy of the point mass. A portion of the mechanical energy is lost during the walking half-cycle due to the inelastic collision of the foot with ground [3], and the rest of the accumulated energy continues to interchange between kinetic and potential energy in the next half-cycle which is described by the percentage of recovery parameter [4].

Although those models are simplified representations of the real human body anatomy, they provide a convenient way to interpret and analyze majority of relevant parameters of the gait cycle. Integral features of the human gait cycle, such as the overall kinetic energy, potential energy, angular momentum with respect to the ground contact point, center of mass trajectory and laws of motion, and ground force in sagittal plane, can be considered using a simplified model (e.g. MSIP).

Using the state space model (1), the ground force can be obtained (Figure 4) and can be used to qualitatively predict the real ground reaction force which occurs during bipedal walking.

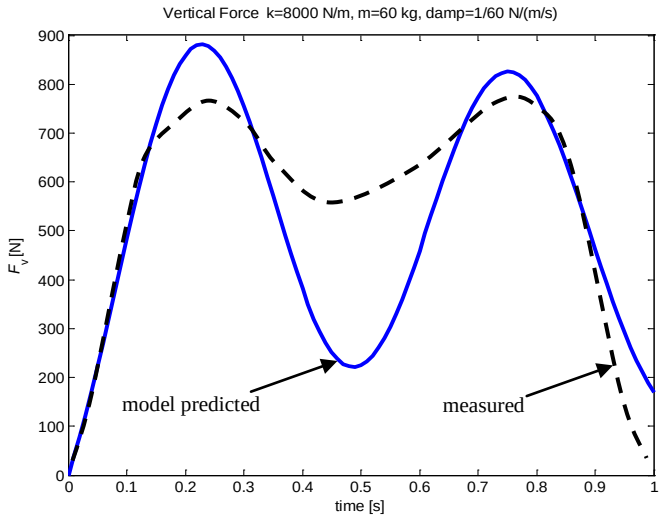

Figure 4. Ground reaction force (vertical component) obtained using the mass-spring inverted pendulum model (including a damper) compared to the real ground reaction force occurring during a single leg stance phase, measured using force plates [9]

Besides the ground reaction force, the mass-spring model can predict qualitatively potential, kinetic and total mechanical

energy of walking. Figure 5 shows the energy change during walking predicted by the mass-spring model.

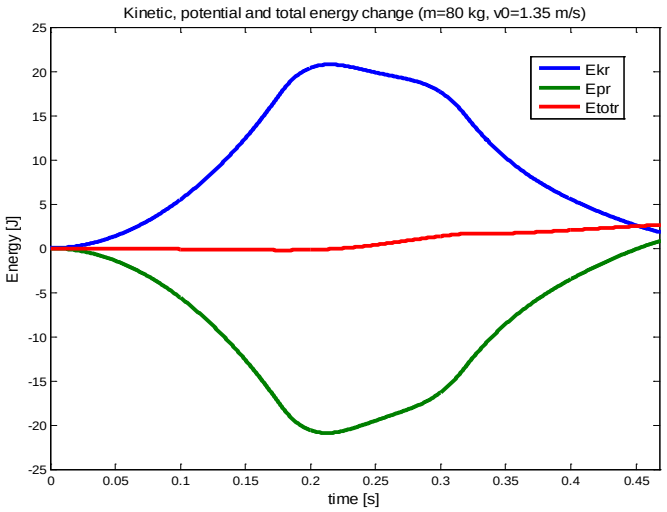

Figure 5. Potential, kinetic and total mechanical energy change (relative energy with respect to the initial energy level)

1.2 Models with Distributed Mass and Multiple DOF

Complex bipedal walking models and their practical implementation to bipedal robots are generally based on human body anatomy [5, 6, 7]. However, all those models and implementations include fewer degrees of freedom (DOF) of motion than the DOF existing in the human body. The spinal region of the body has a high number of DOF. The motion within the spinal region influences the walking cycle behavior, but this motion can be neglected and the majority of models with distributed mass represent the trunk region as a rigid body or as two rigid bodies with a single revolute joint in the trunk. The human body symmetry plane is called the sagittal plane. Dominant accelerations of the body segments centers of gravity occur parallel to the sagittal plane which results in dominant inertial forces and moments due to the motion parallel to this plane. Unless there is a sharp change in the walking direction, relatively negligible inertial forces occur due to accelerations perpendicular to this plane during the walking cycle.

Due to the dominance of the inertial forces parallel to the sagittal plane and for the sake of the model simplification, the analysis and control design shown in this paper is restricted on the planar motion of the model/bipedal robot.

2. Bipedal Robot Model with 10 DOF

The model shown in Figure 6 is a bipedal structure with 10 internal rotational degrees of freedom. Three additional degrees are an absolute (external) rotational degree, which is chosen to be the angle of the trunk with respect to the vertical direction, and two translational degrees with a reference point which is chosen to be at the hip joint. Human joints allow much more freedom than just a rotation about a single axis (a revolute joint). Generally, human ankle and hip joints can be considered as spherical (ball and socket) joints. The knee joint can be approximately considered as a revolute joint (one DOF). However, the model shown in Figure 6 includes only revolute joints, since the analysis is restricted to sagittal plane motion.

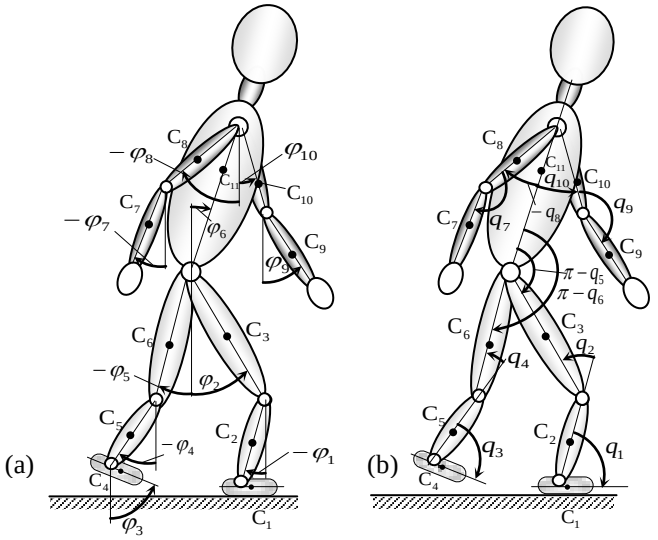

Figure 6. Model with distributed mass: (a) absolute angles, (b) generalized coordinates (angles are relative - joint coordinates)

As described earlier, the spinal region, including the neck and had, is considered as a rigid body, since there is no significant bending during the gait cycle and, consequently, the joint trajectories and generalized forces are not affected significantly.

External coordinates of the hip joint are dependent (assuming no-slip condition) on the other generalized coordinates (angles) of lower extremities within a walking cycle. However, they are still needed to cope with possibility of the walking - running transition.

Two types of coordinates are shown in Figure 6: absolute and relative. Generally, it is easier to work with the absolute coordinates (angles) when we consider the mathematical description of the model's behavior and response to the input torques and forces. However, the joint sensors (e.g. encoders, potentiometers) measure relative angles, which are then directly used in a feedback fashion to guide and control the robot.

Special attention is given in the model to the foot design (Figure 7) in such way that the transition phase between the walking cycles becomes as smooth as possible. A walking robot flat foot design requires that the foot is always parallel to the ground during the stance phase, which is significantly different than the human walking stance phase. Although a flat foot design is commonly used in walking robotics, it causes

certain discontinuities in the kinematic relations and sudden changes in the nominal generalized forces, required to mimic a human-like walking. Besides that, the stabilization of the walking cycle becomes difficult, since the contact is theoretically at the edge of the foot during the significant part of the cycle time. Consequently, the zero moment point (ZMP) is then tied to the foot edge, which complicates the control operations.

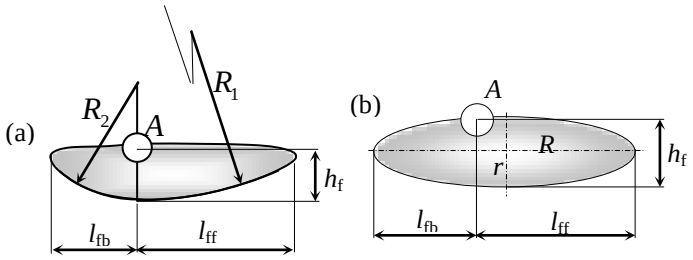

Figure 7. Foot design: (a) two cylindrical surfaces with different radii, (b) ellipsoidal cylinder (the ankle joint is marked by *A*).

2.1 Kinematic and Dynamic Analysis of the Model

Forward kinematics calculates Cartesian coordinates of any point of the structure for a given set of the joint and the external variables. The kinematic relations are necessary to close the set of differential equations that describes the robot dynamics.

The forward kinematics of the robot model can be expressed as follows:

$$\begin{bmatrix} P_{C1} \\ P_{C2} \\ \vdots \\ P_{C11} \end{bmatrix} = f\left(\begin{bmatrix} q_1 & q_2 & \cdots & q_{13} \end{bmatrix}^T\right), \qquad (2)$$

where P_{Ci} (i=1, ..., 11) are position vectors of the center of gravity of the ith segment and has the form $\begin{bmatrix} x_{Ci} & y_{Ci} & 0 \end{bmatrix}^T$. Generalized coordinates in right hand-side of (2) can be the absolute angles of the segment and external coordinates, or they can represent the joint angles and external coordinates. Besides the equation (2), complete kinematic analysis includes the first and second time derivative of (2). Since the expanded equations in (2) and its first two time derivatives are too long to be shown in this paper, they are omitted and we proceed with the dynamic analysis.

Since the control law, which is discussed in the following text, is based on an inverse model and an error dynamics, it is necessary to analyze both forward and inverse dynamic equations. The derivation of those equations is done using the Lagrange energy based method. The inverse model has to provide the nominal generalized forces (the joint torques), based on the nominal joint angular trajectories, which is, by definition, the inverse dynamics. On the other hand, the error based controller uses the differential equations of motion to generate a correction value/signal for the input torques. The differential equations are also needed for numerical simulation of the robot and evaluation of the controller performance.

Figure 8 shows a partial free-body diagram, which includes the right standing leg only.

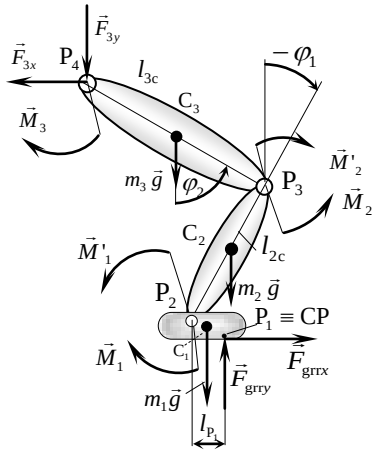

Figure 8. Planar partial free-body diagram for the right standing leg

Besides the reaction forces/torques from the rest of the system, the set of external forces/torques for the subsystem of the support leg during the single support phase includes the torques at the joints, since they perform work and influence the mechanical energy distribution. Such approach is convenient for application of the Lagrange method which provides the way to analyze the relevant forces/torques, without necessity to calculate the internal forces, such as the internal forces at the joints.

The Lagrange equations for the walking robot model have the following form:

$$\frac{\mathrm{d}}{\mathrm{d}t}\frac{\partial L(t,q_\mathrm{i},\dot{q}_\mathrm{i})}{\partial \dot{q}_\mathrm{r}} - \frac{\partial L(t,q_\mathrm{i},\dot{q}_\mathrm{i})}{\partial q_\mathrm{r}} + \frac{\partial R(t,q_\mathrm{i},\dot{q}_\mathrm{i})}{\partial \dot{q}_\mathrm{r}} = Q_\mathrm{r}^{\mathrm{nc}}(t,q_\mathrm{i},\dot{q}_\mathrm{i}), \qquad (3)$$

where $L(t,q_\mathrm{i},\dot{q}_\mathrm{i}) = E_K(t,q_\mathrm{i},\dot{q}_\mathrm{i}) - E_P(t,q_\mathrm{i})$ is the Lagrange function generally depending on time, generalized coordinates and generalized velocities, $R(t,q_\mathrm{i},\dot{q}_\mathrm{i})$ is the dissipation (Rayleigh's**)** function and $Q^{\mathrm{nc}}(t,q_\mathrm{i},\dot{q}_\mathrm{i})$ is the generalized force. The dissipation function can be used to model the lost of energy at the instant of feet collision with the ground. The generalized forces are torques generated by motors at the robot joints.

Kinetic energy of the structure is the sum of the kinetic energy for translational and rotational motion for each segment

$$E_K = \sum_{i=1}^{11}\left(m_i \frac{v_{Ci}^2}{2} + I_{Ci} \frac{\omega_i^2}{2} \right), \quad (4)$$

where v_{Ci} is the i[th] segment center of gravity velocity magnitude, I_{Ci} is the i[th] segment moment of inertia for the center of gravity C_i and ω_i is the angular velocity of the i[th] segment. The centers of gravity velocity can be expressed in terms of the joint angular velocities using the kinematic relations (2). The potential energy is basically the gravitational potential energy since no springs are included in the model.

An alternative way to derive the model dynamics is to apply the combination of the Newton's and Euler-D'Alembert's law for the translation and rotation, respectively. In either way, the following form of dynamic equations is obtained

$$[M(\varphi)][\ddot{\varphi}] + [C(\varphi,\dot{\varphi})][\dot{\varphi}] + [G(\varphi)] = [D(\varphi)][\tau], \quad (5)$$

where: $\varphi = [\varphi_1 \quad \varphi_2 \quad \varphi_4 \quad \varphi_5 \quad \varphi_6]^T$ is the vector of the absolute angles (the foot dynamics has been neglected), $[M(\varphi)]$ is the matrix of inertia, $[C(\varphi,\dot{\varphi})]$ represents cross-correlation of the segments angular velocities, $[G(\varphi)]$ is the gravity influence vector, $[\tau]$ is the control torque vector, and $[D(\varphi)]$ represents the matrix of the control torques distribution.

Although the equations are implemented in the simulation model for the full model (10 DOF), the equations and analysis that are shown here are for the reduced model, for which the arms are considered sufficiently light such that their dynamics is not significant for the system stability. Similarly, the dynamics of the swing leg foot is neglected and the mass is considered lumped at the ankle.

The kinetic energy function for the model is

$$E_K = \tfrac{1}{2}\dot{\varphi}_1^2\left(m_2 l_{1d}^2 + I_2 + \left(2m_3 + m_2^{'} + m_4\right)l_1^2\right) + \\ + \tfrac{1}{2}\dot{\varphi}_2^2\left(m_3 l_{2d}^2 + I_3 + \left(2m_3 + m_2^{'} + m_4\right)l_2^2\right) +$$

The symmetric matrix of inertia is the following:

$$M(:,1) = \begin{bmatrix} m_2 l_{1d}^2 + I_2 + (2m_3 + m_2^{'} + m_4)l_1^2 \\ ((m_2^{'} + m_3 + m_4)l_1 l_2 + m_3 l_1 l_{2d})c_{21} \\ -m_2^{'} l_1 l_{1u} c_{41} \\ -(m_3 l_1 l_{2u} + m_2^{'} l_1 l_2)c_{51} \\ m_4 l_1 l_{3d} c_{61} \end{bmatrix},$$

$$+ \tfrac{1}{2}\dot{\varphi}_4^2\left(m_2^{'} l_{1u}^2 + I_2\right) + \tfrac{1}{2}\dot{\varphi}_5^2\left(m_3 l_{2u}^2 + I_3 + m_2^{'} l_2^2\right) + \quad (3a)$$
$$+ \dot{\varphi}_1\dot{\varphi}_2 c_{21}\left((m_2^{'} + m_3 + m_4)l_1 l_2 + m_3 l_1 l_{2d}\right) -$$
$$- \dot{\varphi}_1\dot{\varphi}_5 c_{51}(m_3 l_1 l_{2u} + m_2^{'} l_1 l_2) - \dot{\varphi}_2\dot{\varphi}_5 c_{52}(m_3 l_1 l_{2u} + m_2^{'} l_2^2) -$$
$$- \dot{\varphi}_1\dot{\varphi}_4 c_{41} m_2^{'} l_1 l_{1u} - \dot{\varphi}_2\dot{\varphi}_4 c_{42} m_2^{'} l_2 l_{1u} + \dot{\varphi}_4\dot{\varphi}_5 c_{54} m_2^{'} l_2 l_{1u} +$$
$$+ \dot{\varphi}_1\dot{\varphi}_6 c_{61} m_4 l_1 l_{3d} + \dot{\varphi}_2\dot{\varphi}_6 c_{62} m_4 l_2 l_{3d} + \tfrac{1}{2}\dot{\varphi}_6^2\left(m_4 l_{3d}^2 + I_4\right),$$

where $c_{ij} = \cos(\varphi_i - \varphi_j)$, (i, j =1,2,4,5,6), m_i is the i[th] segment mass, $m_2^{'}$ is the foot-lower leg combined mass, l_{iu} and l_{id} are the i[th] segment center of gravity position lengths with respect to the neighboring upper and lower joints, respectively, l_i is the i[th] segment length, I_i is the i[th] segment moment of inertia with respect to the axis perpendicular to the sagittal plane.

The potential energy function is

$$E_P / g = \left(m_2 l_{1d} + (2m_3 + m_4 + m_2^{'})l_1\right)c_1 + \\ + \left(m_3 l_{2d} + (m_3 + m_4 + m_2^{'})l_2\right)c_2 - m_2^{'} l_{1u} c_4 - \quad (3b)$$
$$- (m_3 l_{2u} + m_2^{'} l_2)c_5 + m_4 l_{3d} c_6,$$

where $c_i = \cos(\varphi_i)$, (i=1,2,4,5,6).

Rayleigh's dissipation function reflects the energy lost due to the viscous friction in the joints and has the following form for the model

$$R = \tfrac{1}{2}\left(b_1\dot{\varphi}_1^2 + b_2(\dot{\varphi}_2 - \dot{\varphi}_1)^2 + b_3(\dot{\varphi}_6 - \dot{\varphi}_2)^2\right) + \\ + \tfrac{1}{2}\left(b_2(\dot{\varphi}_5 - \dot{\varphi}_4)^2 + b_3(\dot{\varphi}_6 - \dot{\varphi}_5)^2\right), \quad (3c)$$

where b_i (i=1,2,3) are the friction coefficients for the ankle, knee and hip joints, respectively.

The final equations in the form (5) are obtained using the energy based method and the matrices/vectors denoted in (5) are as follows.

$$M(:,2) = \begin{bmatrix} ((m_2^{'} + m_3 + m_4)l_1 l_2 + m_3 l_1 l_{2d})c_{21} \\ m_3 l_{2d}^2 + I_3 + (m_3 + m_2^{'} + m_4)l_2^2 \\ -m_2^{'} l_2 l_{1u} c_{42} \\ -(m_3 l_2 l_{2u} + m_2^{'} l_2^2)c_{52} \\ m_4 l_2 l_{3d} c_{62} \end{bmatrix}$$

$$M(:,3:5)=\left[\begin{array}{c|c|c} -m_2'l_1l_{1u}c_{41} & -(m_3l_1l_{2u}+m_2'l_1l_2)c_{51} & m_4l_1l_{3d}c_{61} \\ -m_2'l_2l_{1u}c_{42} & -(m_3l_2l_{2u}+m_2'l_2^2)c_{52} & m_4l_2l_{3d}c_{62} \\ m_2'l_{1u}^2+I_2 & m_2'l_2l_{1u}c_{54} & 0 \\ m_2'l_2l_{1u}c_{54} & m_3l_{2u}^2+I_3+m_2'l_2^2 & 0 \\ 0 & 0 & I_4+m_4l_{3d}^2 \end{array}\right]$$

The matrix $C(\varphi,\dot{\varphi})$ is given in segments as follows:

$$C(:,1)=\begin{bmatrix} b_1+b_2 \\ -b_2+((m_2'+m_3+m_4)l_1l_2+m_3l_1l_{2d})s_{21}\dot{\varphi}_1 \\ -m_2'l_1l_{1u}s_{41}\dot{\varphi}_1 \\ -(m_2'l_1l_2+m_3l_1l_{2u})s_{51}\dot{\varphi}_1 \\ m_4l_1l_{3d}s_{61}\dot{\varphi}_1 \end{bmatrix},$$

$$C(:,2)=\begin{bmatrix} -b_2+((m_2'+m_3+m_4)l_1l_2+m_3l_1l_{2d})s_{21}\dot{\varphi}_2 \\ b_2+b_3 \\ -m_2'l_2l_{1u}s_{42}\dot{\varphi}_2 \\ -(m_2'l_2^2+m_3l_2l_{2u})s_{52}\dot{\varphi}_2 \\ -b_3+m_4l_2l_{3d}s_{62}\dot{\varphi}_2 \end{bmatrix},$$

$$C(:,3)=\begin{bmatrix} m_2'l_1l_{1u}s_{41}\dot{\varphi}_4 \\ m_2'l_2l_{1u}s_{42}\dot{\varphi}_4 \\ b_2 \\ -b_2+m_2'l_2l_{1u}s_{54}\dot{\varphi}_4 \\ 0 \end{bmatrix},$$

$$C(:,4:5)=\left[\begin{array}{c|c} (m_2'l_1l_2+m_3l_1l_{2u})s_{51}\dot{\varphi}_5 & -m_4l_1l_{3d}s_{61}\dot{\varphi}_6 \\ (m_2'l_2^2+m_3l_2l_{2u})s_{52}\dot{\varphi}_5 & -b_3-m_4l_2l_{3d}s_{62}\dot{\varphi}_6 \\ -b_2-m_2'l_2l_{1u}s_{54}\dot{\varphi}_5 & 0 \\ b_2+b_3 & -b_3 \\ -b_3 & 2b_3 \end{array}\right],$$

where $s_{ij}=\sin(\varphi_i-\varphi_j)$, (i, j=1,2,4,5,6).

The gravity vector $G(\varphi)$ is as follows:

$$G=\begin{bmatrix} (m_2l_{1d}+(2m_3+m_4+m_2')l_1)s_1 \\ (m_3l_{2d}+(m_3+m_4+m_2')l_2)s_2 \\ -m_2'l_{1u}s_4 \\ -(m_3l_{2u}+m_2'l_2)s_5 \\ m_4l_{3d}s_6 \end{bmatrix}g,$$

where $s_i=\sin(\varphi_i)$, (i=1,2,4,5,6), and g is the gravity acceleration.

The torques distribution matrix $D(\varphi)$ is, actually, a constant matrix as follows:

$$D=\begin{bmatrix} 1 & 1 & 0 & 0 & 0 \\ 0 & -1 & -1 & 0 & 0 \\ 0 & 0 & 0 & 1 & 0 \\ 0 & 0 & 0 & -1 & -1 \\ 0 & 0 & 1 & 0 & 1 \end{bmatrix}.$$

Finally, the joints torques vector is

$\tau=\begin{bmatrix}\tau_1 & \tau_2 & \tau_4 & \tau_5 & \tau_6\end{bmatrix}^T$, that has components corresponding to joints torques in the following order: right ankle, right knee, right hip, left knee, left hip, respectively. Again, the swing leg ankle torque is neglected, as well as the dynamics of the swing leg foot.

The equations of the form (5) will be used to derive the control law for each actuated joint of the robot model. This is shown in the following controller design section.

2.2 Controller Design

The controller design is based on a nonlinear system control approach. A combination of the inverse plant with modified gain scheduling is applied.

2.2.1 Desired Robot Motion

Based on typical human walking, the corresponding angular trajectories for the hip, knee and ankle joints can be recorded using cameras and markers positioned on human body segments. In this way, following trajectories are obtained and used for the desired robot motion (Figure 9).

The figure shows that the trajectories do not vary on the left side of the interval as much as they vary on the rest of the walking cycle. The subinterval (the swing phase) contains relatively high derivatives and it is very important to determine precisely the toe off instant, since any variation the toe off instant would cause significant change in the nominal

torques and the calculated ground reaction force. From the mechanical structure basis, there is a configuration change since the structure changes from the double support, which represents the structure with a closed loop, to the single support configuration, which is an open chain configuration.

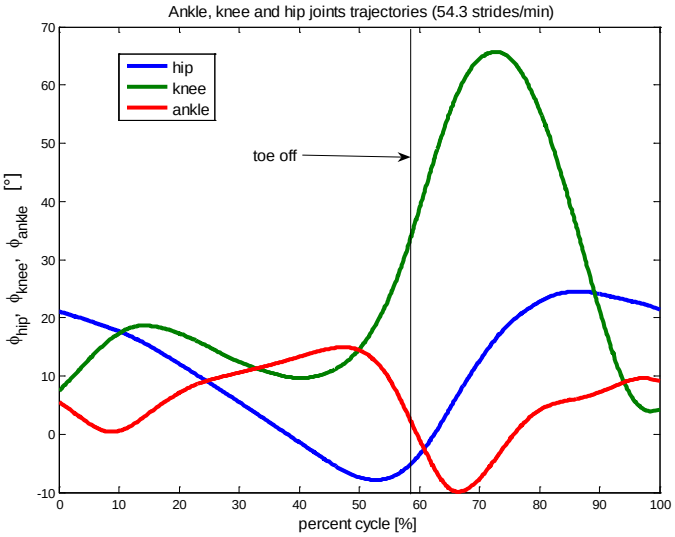

Figure 9. The robot joint trajectories based on a human walking cycle (positive angles denote flexion/dorsiflexion)

Therefore, the when the configuration change occurs it triggers the control law change. Basically, the instant of this configuration change can be determined based on the ground force reaction which is measured using pressure pads positioned at the feet.

The first two derivatives of the desired trajectories are shown in Figure 10 and Figure 11, respectively. Relatively high derivatives are noticeable in the swing phase of the cycle. The nominal trajectories recorded based on human motion usually have significant noise embedded due to errors during the measurements.

Since the control system input requires nominal angular velocity and nominal angular acceleration per each actuated joint, it is necessary to smooth out the nominal trajectories.

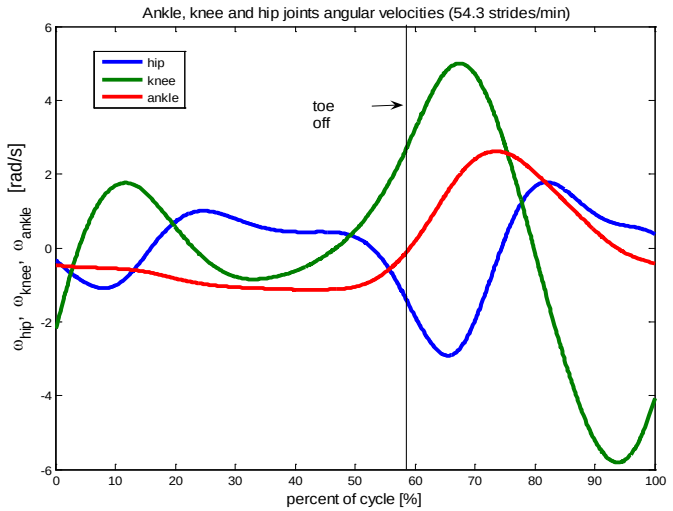

Figure 10. The hip, knee and ankle joint angular velocities

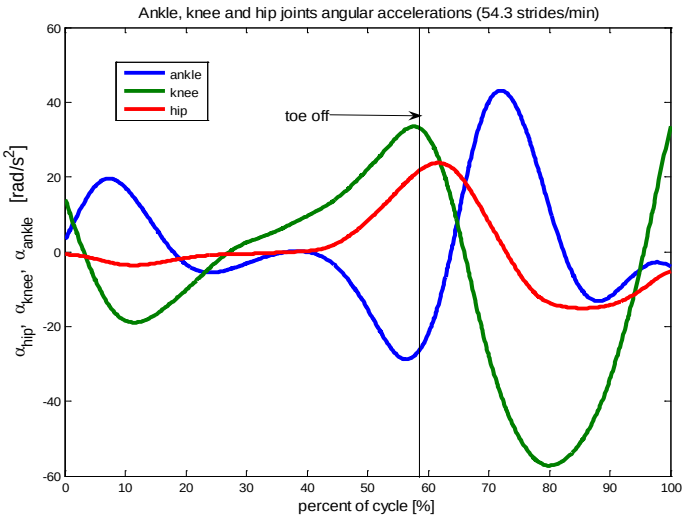

Figure 11. The hip, knee and ankle joint angular accelerations

Although the amplitude of the noise is usually small relative to the nominal signal, its derivatives can dominate the nominal angular velocities and accelerations, which would cause significant errors in the desired motion (errors in the reference input vector).

This problem can be solved using filtering of the recorded signal. The cut-off frequency should be set-up such that the steepest parts of the nominal trajectory can pass through the filter without significant change. In this case, the low-pass filter cut-off frequency was 30 rad/s, for the joint trajectories and their first derivatives.

The nominal trajectories are used for the inverse dynamics to generate nominal torques at the joints, which is discussed next.

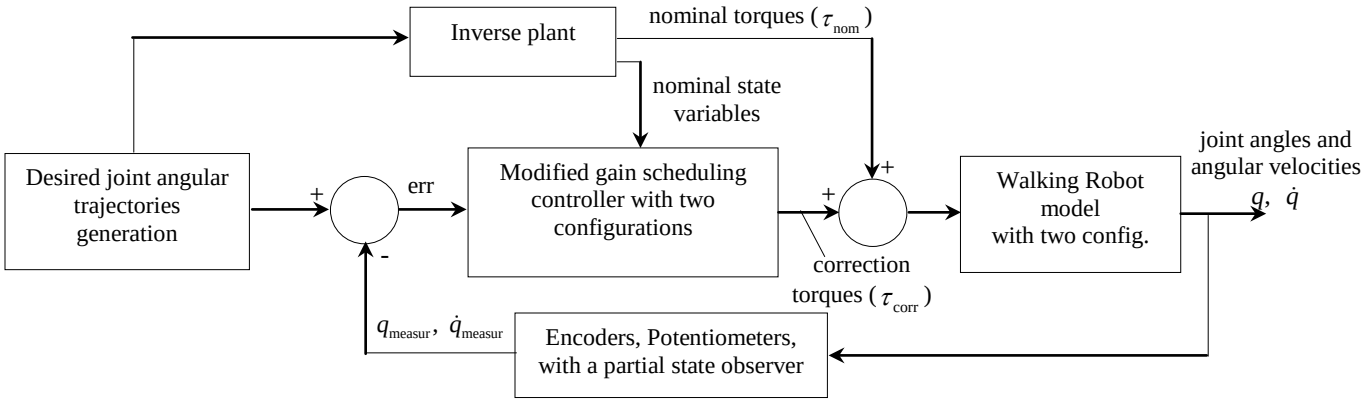

Figure 12. The nonlinear system control based on a gain scheduling approach and the inverse plant

2.2.2 Inverse System

The inverse plant (Figure 12) takes the desired joint trajectories and corresponding derivatives and provides the nominal torques, based on the inverse dynamics equation formed using (5)

$$[\tau] = [D(q)]^{-1}\{[M(q)][\ddot{q}] + [C(q,\dot{q})][\dot{q}] + [G(q)]\}. \quad (6)$$

One significant problem with the inverse plant design is that the derivatives of the desired trajectories (desired output) include the points placed at future time instants, which makes the control system non-causal. A possible solution to this problem is to use an estimator by setting up a Hurwitz polynomial. However, the inverse plant may become unstable using this predictor. In the frame of this work, back-stepping method has been used to stabilize the inverse plant.

2.2.3 Error Dynamics

The nominal inputs to the plant (nominal torques), generated by the inverse plant, are sufficient to drive an ideal system precisely to follow the desired joint trajectories. However, a mathematical representation has always more or less errors with respect to the system which is represented by that model.

Disturbances can appear due to:
- initial conditions,
- effects which are not included in the model, since their way of action and the system response on them is unknown,
- unavoidable delay in sensors (encoders, potentiometers and A/D conversion),
- intentionally simplifying the model mathematical description, since we rely on the control law to minimize the error, (e.g. leaving some friction effect not modeled), etc.

The robot model architecture in the anatomical position has a vertical plane of symmetry (sagittal plane). Due to this symmetry, and cyclic nature of the nominal trajectories, the leg and arm joints on one side of the body have same nominal torques over the walking cycle, just shifted in phase, when the motion is restricted to the planar motion.

Then, the control design of two single support phases and a double support phase completing a walking cycle can be narrowed down to a single support and a double support phase.

Moreover, for the sake of the simplicity of this discussion, the influence of the arms relative dynamics with respect to the trunk will be neglected and considered as a disturbance whose effect has to be minimized by the controller. The system (walking robot mathematical model) can be represented as follows. The state space representation of the three joint variables on the one leg of the robot model is

$$\begin{bmatrix}\dot{\xi}_1\\ \dot{\xi}_2\\ \dot{\xi}_3\\ \dot{\xi}_4\\ \dot{\xi}_5\\ \dot{\xi}_6\end{bmatrix} = \begin{bmatrix}\dot{\theta}_1\\ \ddot{\theta}_1\\ \dot{\theta}_2\\ \ddot{\theta}_2\\ \dot{\theta}_3\\ \ddot{\theta}_3\end{bmatrix} = \begin{bmatrix}\xi_2\\ f_2(\xi)\\ \xi_4\\ f_4(\xi)\\ \xi_6\\ f_6(\xi)\end{bmatrix} + \begin{bmatrix}0 & 0 & 0\\ b_{21}(\xi) & b_{22}(\xi) & b_{23}(\xi)\\ 0 & 0 & 0\\ b_{41}(\xi) & b_{42}(\xi) & b_{43}(\xi)\\ 0 & 0 & 0\\ b_{61}(\xi) & b_{62}(\xi) & b_{63}(\xi)\end{bmatrix}\begin{bmatrix}\tau_1\\ \tau_2\\ \tau_3\end{bmatrix}, \quad (7)$$

or in simplified notation

$$[\dot{\xi}] = [f(\xi)] + [b(\xi)][\tau], \quad (8)$$

where ξ is the state space vector related to the three joint angles and it's derivative, as shown in (7). Although the torques distribution functions $b_{ij}(\xi)$ (i=1, ... , 6; j=1, 2, 3) are shown to depend on entire state vector, precisely they depend on just even components of the state vector (on the angles of

the structure, not angular velocities). Further on, (8) will be used instead of (7) for the sake of simplicity.

The real state space vector of the system is ξ, which generally deviates from the nominal state vector $\bar{\xi}$. The difference of the two vector is denoted as the error vector $\tilde{\xi} = \xi - \bar{\xi}$. Using the time derivative of the error vector and (8), following is obtained

$$\dot{\tilde{\xi}} = \dot{\xi} - \dot{\bar{\xi}} = f(\xi) + b(\xi)\tau - f(\bar{\xi}) - b(\bar{\xi})\bar{\tau} =$$

$$= f(\tilde{\xi} + \bar{\xi}) + b(\tilde{\xi} + \bar{\xi})(\tilde{\tau} + \bar{\tau}) - f(\bar{\xi}) - b(\bar{\xi})\bar{\tau} =$$

$$= \left(f(\tilde{\xi} + \bar{\xi}) - f(\bar{\xi})\right) + \left(b(\tilde{\xi} + \bar{\xi})(\tilde{\tau} + \bar{\tau}) - b(\bar{\xi})\bar{\tau}\right) \approx$$

$$\approx \left.\frac{\partial f(\xi)}{\partial \xi}\right|_{\xi=\bar{\xi}} \tilde{\xi} + \left.\frac{\partial b(\xi)}{\partial \xi}\right|_{\xi=\bar{\xi}} \tilde{\xi}\bar{\tau} + b(\xi)\Big|_{\xi=\bar{\xi}} \tilde{\tau} \text{ , i.e.}$$

$$\dot{\tilde{\xi}} \approx A(\bar{\xi})\tilde{\xi} + b_{\mathrm{d}}(\bar{\xi})\tilde{\xi}\bar{\tau} + b(\bar{\xi})\tilde{\tau} . \qquad (9)$$

Equation (9) is used for the linearization based controller design, where the matrices $A(\bar{\xi})$ and $b_d(\bar{\xi})$ contain the derivatives which are used for the scheduled gains of the controller. The gain scheduled controller, based on (9) alone, cannot cope with the steady state errors. This is the reason why the state space vector $\tilde{\xi}$ is augmented with three integrators (they integrate the angle error for the ankle, knee and hip joint, respectively) as follows

$$\tilde{\xi}_{\mathrm{aug}} = \begin{bmatrix} \tilde{\xi} & \varsigma_1 & \varsigma_2 & \varsigma_3 \end{bmatrix}^{\mathrm{T}}, \text{ and}$$

$$\dot{\tilde{\xi}}_{\mathrm{aug}} = \begin{bmatrix} \dot{\tilde{\xi}} \\ \dot{\varsigma}_1 \\ \dot{\varsigma}_2 \\ \dot{\varsigma}_3 \end{bmatrix} = \begin{bmatrix} A(\bar{\xi})\tilde{\xi} + b_{\mathrm{d}}(\bar{\xi})\tilde{\xi}\bar{\tau} + b(\bar{\xi})\tilde{\tau} \\ \tilde{\xi} \\ \tilde{\varsigma}_1 \\ \tilde{\varsigma}_2 \end{bmatrix}. \qquad (10)$$

Stability of the gain scheduling controller is limited by the maximum allowed time derivatives of the desired joint angle trajectories, which are used as the scheduling variables

$$\left\| \dot{q}_{\mathrm{des}}(t) \right\| \le \mu , \qquad (11)$$

where $q_{\mathrm{des}}(t)$ is the vector of desired joint angles trajectories and μ is a positive constant (Theorem 12.1 in [14]). This is a serious limitation of the controller as a result of the "frozen time" concept application. However, application of the inverse system (Figure 12) significantly improved the controller capabilities, since the inverse system (plant) includes the time derivatives of the desired joint trajectories and the limitation (11) on the time derivatives of the scheduling variables (desired joint angles) is replaced by the limitation on the time derivatives of the error vector. For this design, μ is about 6 rad/s.

The performance of the gain scheduled controller, combined with the inverse plant, are discussed in the following.

3. Simulation Results

Using the gain scheduling based controller in the way shown in the block diagram of Figure 12, the following results are obtained. Figure 13 shows the nominal torques at the hip, knee and ankle joint, which are obtained using the inverse plant system.

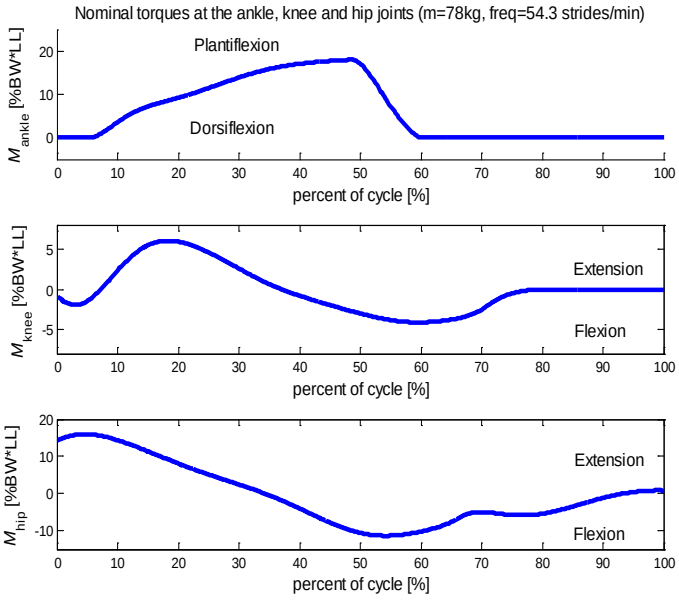

Figure 13. Nominal torques at the ankle, knee and hip joint obtained via the inverse plant of the controller system

These nominal inputs to the controlled system are normalized with respect to the body weight (BW) multiplied by the total leg length (LL), such that the results are scalable with respect to the body mass (if the proportion of the body segments lengths and mass is maintained constant). The tracking performance of the controller for the ankle joint is shown in Figure 14.

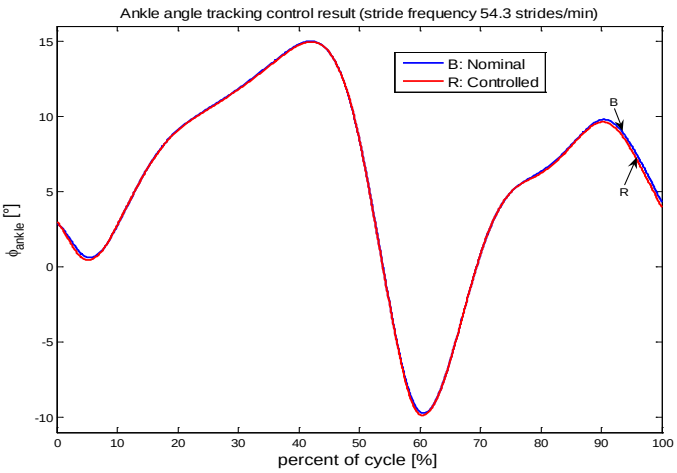

Figure 14. Controller tracking performance for the ankle joint

The controller tracking performance for the knee joint angle is shown in Figure 15.

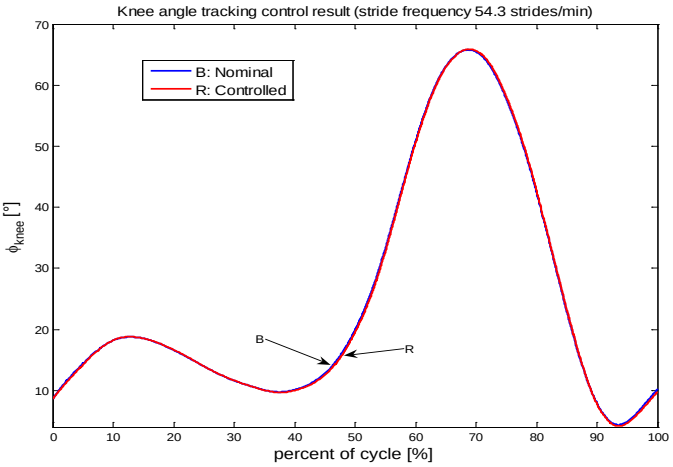

Figure 15. Controller tracking performance for the knee joint angle

For the hip joint, the goal of the controller was a regulation of the trunk angle with the respect to the vertical direction. The controller performance of keeping this angle relatively small during the walking cycle is shown in Figure 16.

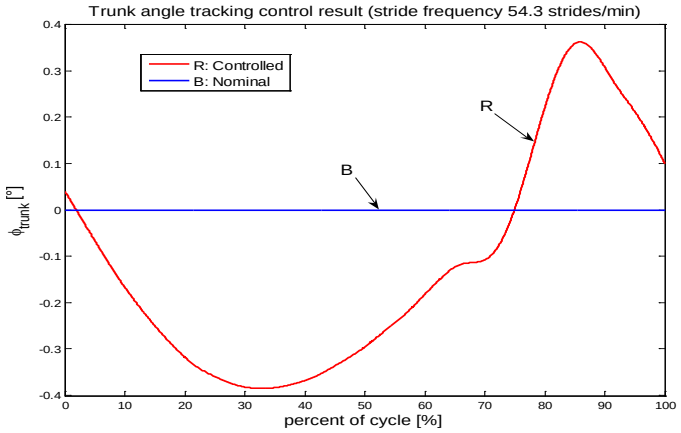

Figure 16. The controller tracking performance of the hip joint angle and regulation performance of the trunk angle via the hip torque

Finally, the ground force from the robot model is calculated and shown in Figure 17. Besides the ground force of the model with distributed mass.

The controller design performance with results shown in the Figures 14 through 17, are discussed next.

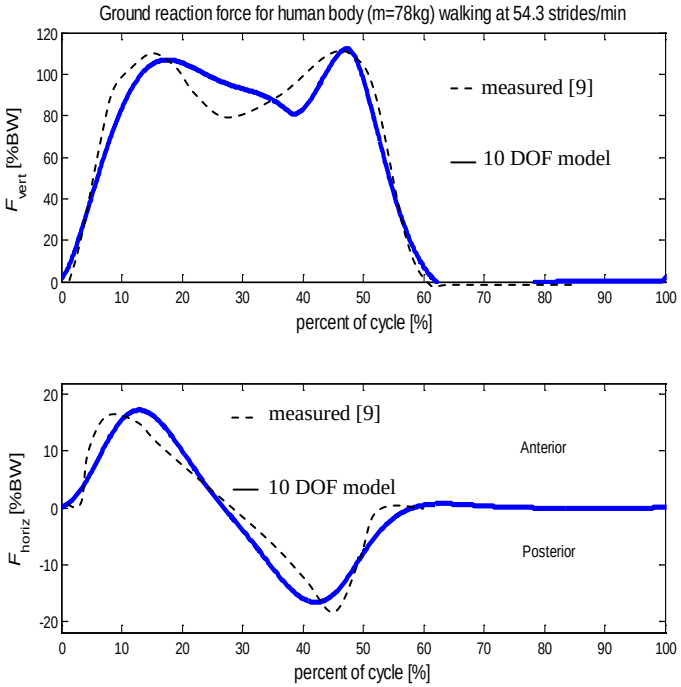

Figure 17. Ground reaction force calculated using the distributed mass model and compared to the measured force using the force plates method [9]

4. Results Discussion

Initial system response with a zero initial conditions (zero angles, which means the standing anatomical position, and zero angular velocities) looked a bit worse than the system response for the second cycle, whose results are shown in the

figures. However, the steady walking cycle response is achieved very fast after the (zero) initial conditions and the second cycle is shown in the figures.

The tracking error for the ankle and knee joints angles is not significant as shown in Figures 14 and 15. Although the time derivatives are very high in a couple of subintervals of the cycle period, the gain scheduled controller succeeds to keep the response angle close to the desired path. The high time derivatives is the always a questionable issue with gain scheduled controllers, since gain scheduled controllers are based on the frozen time concept. Accepting that the time derivatives are relatively high for this type of the control, the successful control performance can be justified in this case by the usage of the inverse plant such that the error dynamics based controller has to correct just a small deviation from the nominal torques provided by the inverse plant.

Although the desired angle trajectories (Figure 9) showed that there is a small variation of the trunk angle with respect to the vertical direction, the control goal for the hip joint was set-up to maintain (regulate) a zero trunk angle. The results shown in the figure indicate a good regulation performance, since the angle variation remains within a 1° range.

Finally, the ground force, calculated based on the centers of gravity acceleration, shows relatively good agreement with the experimentally measured data. Small deviations can be partially explained by eventual deviations of the segmental lengths of the walking model from the real human segments, accompanied with some deviations of the recorded joints angle versus time functions from the real joint angle trajectories.

5. Conclusion

Advanced bipedal robot control techniques rely on an inverted dynamics of the bipedal robot model (reference model). Therefore, it is essential to create a precise but still relatively simple model that will provide accurate calculation of the relevant forces and torques needed to obtain particular set of desired joint trajectories.

Two main groups of the bipedal walking models can be used for this purpose. The first group, concentrated mass at the center of gravity, consists of relatively simple models useful for ground force analysis, kinetic, potential and total energy balance analysis, energy recovered from potential to kinetic and vice-versa. The second group of models consists of models with distributed mass, which allow more detailed analysis such as torques at the walking structure joints (which cannot be measured directly in a human body), inertial effects due to the segmental motion with respect to the center of gravity, and control law design used to guide a bipedal robot.

As a significant simplification of walking models with respect to the human body structure, one can consider the entire spinal region as a rigid body, since there is no significant bending and no significant contribution of the trunk bending dynamics to the overall walking structure dynamics. Other simplifications can be related to the types of the joints and the foot shape.

A walking robot tracking control can be based on human body joint trajectories. Those time-angle functions can be recorded for each joint using cameras, segmental markers and image processing. The control system input requires nominal angular velocity and nominal angular acceleration per each actuated joint. Therefore, it is necessary to smooth the nominal trajectories and pass the trajectories through a low-pass filter, since any discontinuity or a sudden change in the recorded data generates high derivatives and can make the control system unstable.

The cut-off frequency should be setup such that the steepest parts of the nominal trajectory can pass through the filter without significant change. In this case, the low-pass filter cut-off frequency was 30 rad/s, for the joint trajectories and their first derivatives.

A control system can be successfully designed and implemented in a form of a combination of an inverse plant model and a linearization based controller with gain scheduled according to the nominal state space vector change. This is the novel contribution of the current article. The inverse plant generates the nominal control inputs (the joint torques). However, the inverse plant becomes non-causal if precise values of time derivatives of the reference input (desired output) are necessary. Alternatively, the derivatives can be predicted by the inverse plant. A disadvantage of this approach is the fact that the system can become unstable and need to be stabilized. In this work, a back stepping method was used.

The gain scheduled error dynamics controller successfully made the system output follow the desired joint trajectories. Although gain scheduling is a frozen time concept, which means that the absolute values of the time derivatives must stay within a certain range in order to maintain controller performance and stability of the system, the simulation results showed remarkable tracking performance, which can be explained as a good prediction of the nominal torques via the inverse plant.

The comparison of the model results for the ground force shows a satisfactory agreement between the model results and measured data from the literature.

The main problem with traditional control techniques for a bipedal robot is that MIMO systems such as bipedal robots are controlled joint by joint independently and the cross coupling of different input-output pairs is treated as disturbances. These techniques are convenient in the cases when it is difficult to develop a reasonable model of the controlled system, but generally cannot provide high performance in MIMO systems.

Bipedal robots require precise desired trajectories tracking in order to balance during walking steps. The idea proposed in this paper is that those cross couplings can be modeled

precisely, rather then treat them as disturbances, and significantly improve the overall system performance. This article showed a novel nonlinear gain scheduled controller design combined with a concentrated mass reference model.

Modeling the bipedal robot as a MIMO system, rather then considering the system as a number of independent joints with disturbances, means that we consider how the i^{th} actuator/torque influences the j^{th} joint motion, in order to adjust the combination of the torques (inputs), such that the joints follow prescribed joint trajectories.

References

[1] Kuo, A. D., 2007, "The six determinants of gait and the inverted pendulum analogy: A dynamic walking perspective," *Human Movement Science*, **26**, pp. 617-656.

[2] Geyer, H., Seyfarth, A., and Blickhan, R.,2005, "Spring mass running: simple approximate solution and application to gait stability," *J. Theor. Biol.* **232**, pp. 315–328.

[3] Ruina, A., Bertram, J. E., & Srinivasan, M., 2005, "A collisional model of the energetic cost of support work qualitatively explains leg sequencing in walking and galloping, pseudoelastic leg behavior in running and the walk-to-run transition," *Journal of Theoretical Biology*, **237**, pp. 170–192.

[4] Giovanni A. Cavagna, A. G., Heglund, C. N., and Taylor, C. R., 1977, "Mechanical work in terrestrial locomotion: two basic mechanisms for minimizing energy expenditure," *Am J Physiol.*; **233** (5): R243-61.

[5] Honda Motor Co., 2007, "Technical Information," http://world.honda.com/ASIMO.

[6] Shirata, S., Konno, A., and Uchiyama, M., 2004, "Design and development of a light-weight biped humanoid Robot Saika-4," *Proceedings of 2004 IEEE/RSJ International Conference on Intelligent Robots and Systems*, pp. 148-153.

[7] Yamaguchi, J., and Takanishi, A., 1997, "Development of a Leg Part of a Humanoid Robot−Development of a Biped Walking Robot Adapting to the Humans' Normal Living Floor," Autonomous Robots, Vol.43, pp.69-385.

[8] S. Collins, A. Ruina, "A bipedal walking robot with efficient and human-like gait", *Proc. of the IEEE International Conference on Robotics and Automation*, April 18-22, 2005, pp.1983 -1988.

[9] Umberger, R. B., and Martin, E. P., 2007, "Mechanical power and efficiency of level walking with different stride rates," *The Journal of Experimental Biology*, **210**, pp. 3255-326.

[10] Garcia, M., Chatterjee, A., Ruina, A., and Coleman, M., 1998, "The Simplest Walking Model: Stability, Complexity, and Scaling," *Journal of Biomechanical Engineering*, ASME, **120**, pp. 281-288.

[11] Kuo, D. A., 2001, "A Simple Model of Bipedal Walking Predicts the Preferred Speed–Step Length Relationship," *Journal of Biomechanics*, ASME, **123**, pp. 264-269.

[12] Whittington, R. B., and Thelen., G. D., 2009, "A Simple Mass-Spring Model With Roller Feet Can Induce the Ground Reactions Observed in Human Walking," *Journal of Biomechanical Engineering*, ASME, **131**, pp 011013-1 - 011013-8.

[13] Peasgood, M., Cubica, E., and McPhee, J., 2001, **"**Stabilization of a Dynamic Walking Gait Simulation," *Journal of Computational and Nonlinear Dynamics*, ASME, **2**, pp. 65-72.

[14] Khalil, K. H., 1996, "Nonlinear Systems," 2nd Edition, Englewood Cliffs, NJ, Prentice-Hall.